Antibacterial coating for complex orthopedic metal implants

F.M. Dijkmans [4710916]
Master thesis, 3mE, Biomedical Engineering

Supervisor: S. Amin Yavari
Professor: H.H. Weinans

October 2, 2019

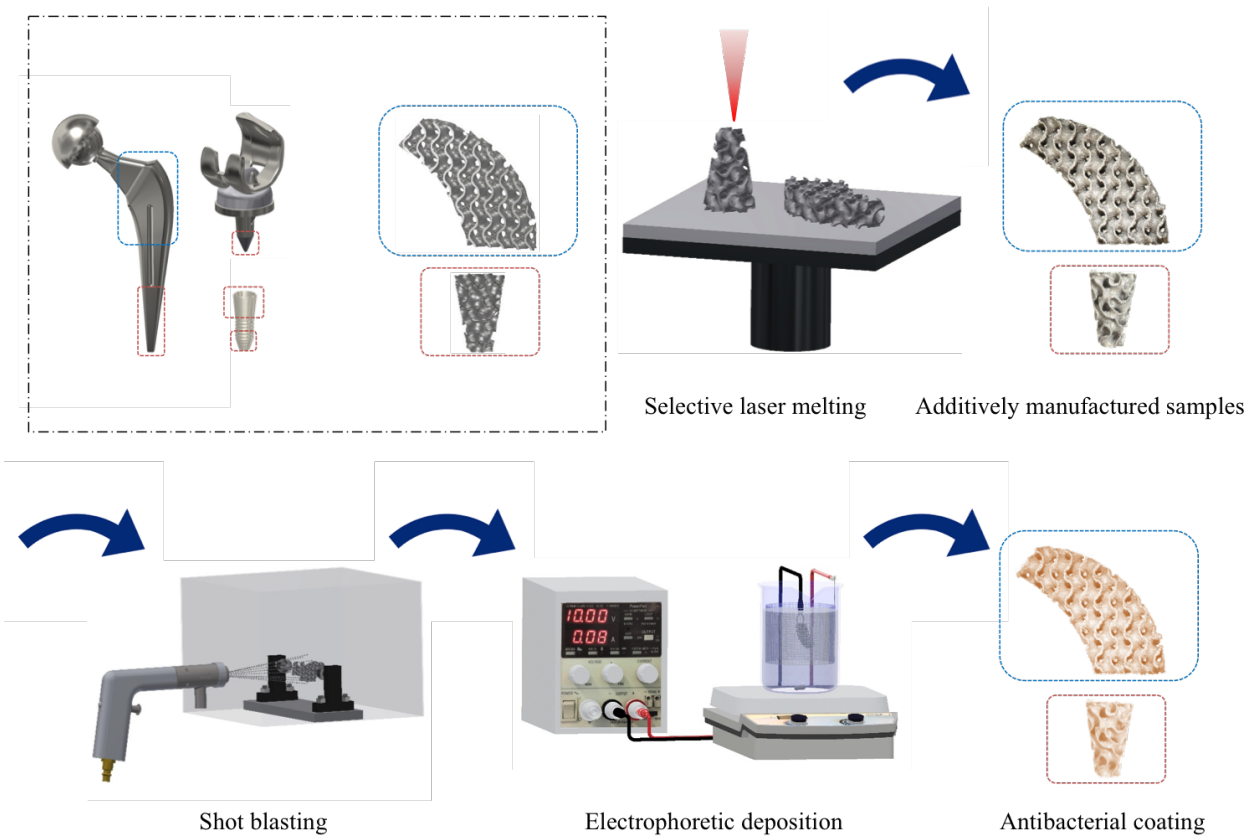

A B S T R A C T:

Prosthetic failure due to implant-associated infections remains a big problem, despite the extensive use of implants and number of researches performed on this topic. A new problem arises with the development of additively manufactured complex orthopedic metal implants. In spite of the advantages that come with patient specific implants to cure the most critical orthopedic situations, these implants are inherent to infection susceptibility. Currently, no study has shown deposition on such complex implants, therefore this research aims to make the first steps towards an antibacterial coating deposited on additively manufactured complex implants to fight peri implant infections. This is facilitated by means of electrophoretic deposition. In order to develop homogeneous deposition of a chitosan/gelatin based coating loaded with vancomycin or gentamicin on titanium implants, a state-of-the-art setup was used, containing a cylindrical counter electrode surrounding the complex specimen. After parameter optimisation, *in vitro* release behaviour, cell viability assays and antibacterial tests were performed, in order to investigate the biological behaviour of the coating. The release behaviour, which was dependent on coating degradation, showed a burst release after one day followed by sustained release up to day seven. Specimen including antibiotics showed antibacterial effect against *S. Aureus*. While all planktonic bacteria where eradicated, biofilm formation by adherent bacteria was significantly decreased, however not prevented. Cell viability assay showed bacterial adherence and growth, with an increased rate in the gentamicin samples, potentially caused by the high hydrophilicity of this drug. While an *in vivo* study is suggested to obtain more in-depth insights in the biological behaviour of the coating, this method is suggested to be a successful way to create a homogeneous coating against peri implant infections on complex implants, preventing peri implant infections, to reduce the change of patient specific implant revision.

Keywords: metal implants, 3D printing, additive manufacturing, antibacterial coatings, electrophoretic deposition, complex orthopedic implants, antibiotic release, patient specific implants

I. Introduction

A. Implant associated infections

IMPLANT associated infections (IAIs) are proven to be one of the most common reasons for orthopedic implant revision. IAIs are especially critical when addressing additively manufactured (3D printed) complex implants. IAIs leading to failure of a prosthetic device, resulting in implant revision are remarkably problematic for orthopedic implants, since they are designed to remain in the body for an unlimited period of time after implantation [1]. In the Netherlands, 13,3% (n=28.639) of all total hip procedures (n=215.380) during the last seven years required revision. Of all revisions, 20,3% were caused by infections, making this the third main reason of failure for orthopedic implants according to LROI annual report 2018 Dutch Arthroplasty Register [2]. Furthermore, a significant increase in the demand of total hip and knee arthroplasty is expectedin the years to come, based on the increase rates of the past decade and due to life expectancy increases [3, 4]. The gram-positive *Staphylococcus Epidermidis (S. Epidermidis)* is the most common bacteria in Europe and *Staphylococcus Aureus (S. Aureus)* in the USA [5]. These bacteria are found at the surgical site of 90% of all implants, originating from contamination during surgery [6]. Implant associated bacteria are not distributed singularly like planktonic bacteria, but tend to tightly adhere to the surface of biomaterials forming an abundant matrix containing extracellular polymeric substances so-called biofilm. Bacteria can reach the implant and colonize during a "race for the surface", which is a process that takes place during the first six hours after implantation [1]. In this critical phase, a contest between bacterial adhesion and tissue cell integration takes place. Bacteria that reach the surface first will form biofilm. In biofilm state, bacteria are 10 to 1000 times more resistant to antibiotics and host response [7]. Therefore, biofilms are mostly responsible for the implant infection persistence and can have vigorous consequences for the patient, including implant revision [1, 7].

B. Additive manufacturing

Nowadays, the focus of orthopedic implant productions and development has shifted to the use of additive manufacturing [8]. Additive manufacturing is a free-form fabrication technique that allows for patient specific implants with the use of Computed Tomography (CT). Such implants include complex porosity and accurate topological designs to improve tissue integration and regeneration resulting in fast recovery and decreased implant revision [7]. Additive manufacturing can be applied with several materials such as polymers, ceramics and metals [8]. Metals are the most widely applied biomaterials in orthopedic surgery [2]. Porous metal implants increase the mechanical behaviour of an implant compared to compact implants, regarding fatigue behaviour and stress shielding. For example, stress can be mitigated, due to the decreased elastic modulus of a metal material. Porous titanium stiffness could additionally change stress and strain distribution within the host tissue, changing the mechanobiological regulation, which can be favorable for bone apposition and patterning [9]. Their mechanical behaviour is comparable to bone, where the porosity varies between 50% and 90% for trabecular bone and 3% to 5% for cortical bone [10]. This porosity in bone causes a specific elastic modulus of 3 to 30 Gpa for cortical bone and 0.02 and 2 Gpa for trabecular bone, which is more comparable to porous metals than rigid structures. Moreover, this allows for permeability, which is ideal for oxygenation and nutrition of cells that reside in the inner spaces of the bone [11]. Additive manufacturing of metals can be achieved by using the selective laser melting technique, a process that fuses metal particles together (layer-by-layer), allowing for specified unit cell variations on a microscopic scale [12]. Different designs of unit cells, including pore size and structure are evaluated and compared in several studies to create the most desirable mechanical behaviour and host response. Gyroid-like unit cells are found to be preferable, since studies have showed that curvature is an important factor for tissue regeneration [11]. The concave surface is found to positively impact tissue regeneration when comparing to flat and convex surfaces [13]. Additionally, this geometrical design has preferable stress and strain variables, which creates a desired mechanical loading architecture, to minimise bone resorption [13].

C. Complex patient specific implants

Complex orthopedic implant surgeries often requires longer and open procedures, not only because of their very complex and varying shapes, but also because most patient specific implants are produces, only in case of critical situations. These situations include spinal surgeries, due to vanishing bone diseases [14] or mandibular reconstruction due to bone cancer removal [15]; thus, cases that cannot be treated using conventional approaches and techniques [2, 14]. The approval of patient specific implants is complicated due to strict medical standards and regulations, which results in complex implants, being exclusively used for very specific and critical situations [14]. Moreover, revision of a porous complex implant is extremely difficult, due to the strong bone-ingrowth after implantation. This increases the urgent need for antibacterial coatings for patient specific implants. In these emergency situations, the patients' general health and quality of bone tissue surrounding the implant can be poor, as bone resorption can be a consequence of osteoarthritis (inflammation of the bone joints) [3, 16]. These factors can result in a prolonged surgical procedure. Since surgery is the most critical moment for implant infection, complex orthopedic implants are inherent to bacteria susceptibility [17].

D. Coating for complex implants

IAIs are considered as very challenging in orthopedics, which is why an antibacterial coating should be developed to prevent early stage infection and development to biofilm. Bacterial infection could also increase the cytotoxicity of metal ions at the implant interface, influencing the general health of the patient. This could increase the chance of revision surgery on the long-term [18]. Despite the fact that coating solutions for this problem

are gaining significant attention, no research has developed an antibacterial coating for complex "patient specific" orthopedic implants. Antibacterial-release coatings that include polymers and are loaded with antibiotics appear to be a suitable candidate to fight peri-implant infection [19]. Previous studies suggest that electrophoretic deposition is a frontier technology for deposition of such coatings [20]. Electrophoretic deposition is fast, cost-effective, site-selective and it is able to produce mechanically resistant and stable coatings with adjustable thicknesses [7]. Material possibilities have been investigated, concluding that co-deposition of the natural polymers chitosan and gelatin could be favourable, due to their excellent biological performance, physical properties, degradation, drug release properties, cost-effectiveness and cell adhesion [19, 21]. Nevertheless, optimization of electrophoretic deposition parameters and setup to create a homogeneous deposition and preferable coating thickness on the complex implants will be challenging.

E. Aim of this study

The aim of this research was to develop an optimised electrophoretic deposition setup that could deposit a homogeneous antibacterial-release coating on complex implants to avoid bacterial adhesion in the most critical stage of bacterial infection. Vancomycin and gentamicin, which are widely used antibiotics and can prevent bacterial adhesion, were loaded in positively loaded polymeric particles. [22–25]. To test the biological response and antibacterial efficiency of the deposited coating, *in vitro* release tests, antibacterial assays and cell viability tests were executed. This study has made the first step towards successful antibacterial coating deposition for additively manufactured complex metal implants.

II. Materials and Methods

A. Design and additive manufacturing

A sheet-Gyroid unit cell was employed as the base for the lattice structure. Initially, a surface profile of a cubic scaffold was generated by k3DSurf software. The resulting file was processed using 3-matic software (Materialise, Belgium), through a combined process of wrapping and boolean intersection with a stem/cone volume structure to create the highly porous structure in a 3D model. These structures were chosen in order to mimic an orthopedic hip implant, with the most highly complex shapes. The designed geometrical and morphological properties of stem and cone specimens are presented in Table I.

The structures were additively manufactured via Selective laser melting (SLM) using a SLM machine equipped with a Twin (2x400W) IPG fiber laser (IPG Photonics Corporation, Oxford, USA) having a wavelength of range 1070 10 nm. SLM processing of Ti6Al4V-ELI powder with a particle size of 20-63 μm (grade 23) from SLM Solution Group (AG, Lubeck, Germany) was performed on top of a solid titanium substrate, with a laser thickness of 30 μm and a scan velocity of 10 m/s in an inert atmosphere with oxygen concentrations below 50 ppm. Afterward, the specimens were cut off the titanium base plate with wire electrical discharge machining. The implants were washed consecutively with acetone, ethanol and ultra-pure water (MilliQ).

B. Surface modification

The metal surface of the implant specimens was modified using a surface treatment method called shot blasting (SB), to obtain desirable characteristics including the elimination of imperfections, fatigue improvement and surface biofunctionalization [26]. With a pistol, Alumina (Al_2O_3) abrasive with an average particle size of 50 micron was fired with high velocity and pressure of 4 Bar in a controlled manner towards the implant surface, in order to remove the partially melted titanium particles that were formed during SLM (fig. S1a). The stem and cone implants

Designed parameters	Stem	Cone
Big radius (*mm*)	24	5
Small radius (*mm*)	21	2,5
High (*mm*)	5	15
Pore size (μm)	892	892
Sheet thickness (μm)	316	316
Porosity (%)	81,5	80,9
Surface area (*mm2*)	2102	1070

TABLE I: Geometrical and morphological design parameters for the stem and cone samples

were shot blasted in a closed cabinet while rotating for 90 seconds, clamped on a needle (fig. S1b). The up and downside of the implants were shot blasted for 45 seconds while holding tightly in front of the shot blasting pistol. After shot blasting, the titanium implants were washed and sonicated in an Ultrasonic bath (Fisherband FB115047) for 30 minutes with 99% Acetone, with 99% Ethanol and MilliQ respectively and left to dry in an oven for eight hours (50 °C). The morphology of the shot blasted surface and non-shot blasted/As Manufactured (AM) implant surface were visualised using a scanning electron microscope (SEM, Jeol, JSM-IT100, Japan).

C. Electrophoretic deposition process and coating parameter optimization

Electrophoretic deposition was applied in order to deposit positively loaded chitosan/gelatin [Chi/Gel] particles on the titanium surface of the implant specimen. The specimen were connected to the negative power supply under a constant voltage mode to create a negative implant surface potential. 0,5 mg/mL chitosan (Low molecular weight, deacetylated chitin, poly(D-glucosamine), Sigma-Aldrich, Germany) and 1,0 mg/mL Gelatin (Porcine skin, Sigma-Aldrich, Germany) were used as coating base, to later incorporate the antibiotics vancomycin hydrochloride (Sigma-Aldrich, Germany) and gentamicin sulphate (Gen) (Sigma-Aldrich, Germany) [16,21].

To optimize the parameters deposition time (t) and voltage (V) for uniform deposition of the coating, different values for voltage and deposition time (obtained from previous EPD studies) were evaluated by adding 0,01 mg/ml Fluorescein isothiocyanate (FITC) to the colloid solution and visualising the coating with a fluorescence microscope (fig. S3a). The optimal parameters were selected according to their homogeneity, morphology and deposition weight. A 1% aqueous acetic acid solution

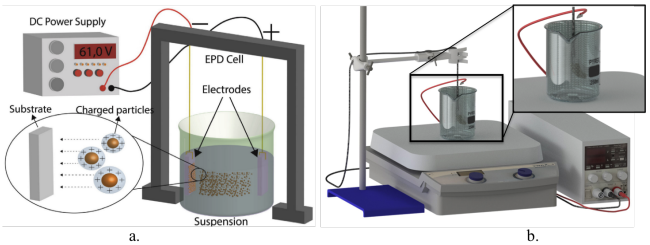

Fig. 1: a) Schematic figure of electrophoretic deposition. (Retrieved from: E. Avcu, F.E. Bastan, H.Z. Abdullah, M.A.U. Rehman, Y.Y. Avcu, A.R. Boccaccini, Electrophoretic deposition of chitosan-based composite coatings forbiomedical applications: A review.Progress in Materials Science (2019)[19] b) Electrophoretic deposition setup used during the experiments including the surrounding anode and the titanium implant as cathode.

was used to dissolve chitosan and gelatin separately. After 24 hours of magnetic stirring, chitosan and gelatin were poured together in a beaker to form the Chi/Gel complexes [21]. 0,01 mg/ml FITC solved in 1 mL ethanol was added in the solution covered with Aluminium foil, one hour before the electrophoretic deposition (EPD) process. For electrophoretic deposition, a cylindrical anode (r = 15mm) was used that surrounded the stem and cone implant specimen during EPD (Fig. 1). The stem and cone implant specimen were connected to the negative power supply to create a cathodic deposition in the DC-EPD setup [27, 28]. To reduce bubble formation at the cathodic implant surface, 100mM hydroxide peroxide (H_2O_2) was added to the colloid solution [29]. To determine the difference of the coating with and without addition of H_2O_2, the coating was stained either with 0,01 mg/mL FITC or with 0,4 mg/mL red dye (New Coccine, Sigma-Aldrich) and visualised using a fluorescence microscope (OlympusBX511) and a stereoscope (Olympus SZ61). After optimisation of the solution parameters, either 0,5 mg/mL vancomycin [Chi/Gel/Van] or 1,0 mg/mL gentamicin [Chi/Gel/Gen] was added to the Chi/Gel solution to create the antibacterial-release coatings on both shot blasted (SB) and (AM) cone and stem specimen. For every implant, 50 mL solution was used in a 50 mL beaker using the cylindrical anode (r=15mm) to deposit the coating for each group similarly, under constant magnetic stirring. After coating optimisation, eight experimental groups for the stem and cone could be separated for the SB and AM implant specimen: As Manufactured (= no coating) [ASM], chitosan/gelatin [Chi/Gel], chitosan/gelatin/vancomycin [Chi/Gel/Van] and chitosan/gelatin/gentamicin [Chi/Gel/Gen] (Table II).

D. Characterisation of the deposited coating

The presence of coating was visualised using red dye (New Coccine, Sigma-Aldrich, Germany) and the morphology of the coating was visualised using FITC. The surface chemistry of the different experimental groups was analysed with energy-dispersive X-ray spectroscopy (EDS-mapping) using a SEM (Jeol JSM-IT100, Japan). A 900X magnification area (fig. S5) was visualised for every SB experimental group to determine the atomic concentration and distribution of the elements present on the implant surface (n=1). The coating weight was obtained by weighing the implants before and after coating deposition (n=3).

E. In vitro release profile

For *in vitro* release measurements, both stem and cone were coated with vancomycin and gentamicin for the AM and SB groups, using the optimised EPD setup and parameters (n=3). The coated specimens were soaked in 1 mL PBS (pH=7.4) for cone specimen and 2 mL PBS (pH=7.4) for stem specimen and incubated at 37 °C. After 2h, 6h and day 1 t/m 7 the PBS was refreshed. 100 μL of every sample was measured with the Fluoroskan Ascent FL Multiplate reader (Thermo Labsystems, Helsinki, Finland) at a wavelength of 544 to determine the cumulative release profile of vancomycin and gentamicin at every specific time point. To measure the concentration of vancomycin, ultra-performance liquid chromatography (UPLC) was employed, using an ACQUITY UPLC H-Class PLUS Bio system (Waters Corporation, US) equipped with a BEH C18 column (1.7 μm, 2.1 mm x 50 mm, Waters). The two mobile phase mixtures used consisted of 100% acetonitrile (ACN) mixed with 0,1% trifluorasic acid (TFA) and 5% ACN (mixed with 95% MilliQ) mixed with 0,1% TFA. A flow rate of 1mL/min was used to elute the samples. A photodiode array detector (PDA) (Waters 2996, Waters, Canada) was used at an absorbance of 233 nm. To analyse the results, the additional PDA dector software was used (Eaters Empower 3 Pro, Waters, Canada). The concentration of gentamicin was measured using UV-Spectroscopy. A Boric acid buffer was prepared by dissolving 24,7 g Boric acid in 900 mL MilliQ. 50% (w/v) of potassium hydride was added to adjust the pH to 10.4 pH. Sufficient water was added to produce 1000 mL solution for accurate pH adjustment. The OPA reagent was prepared by dissolving 0,2 g o-phthaldialdehyde (OPA) (Sigma-Aldrich, Germany) in 1mL isopropanol and added to 19 mL of 0.4 M Boric buffer. To adjust the pH to 10,4 pH, 0,4 ml 2-mercapto-ethanol was added to the solution using potassium hydroxide and finally incubated for 10 minutes at room temperature. The absorbance was measured by spectrophotometrically (Spectrostar Nano, Germany) at 332nm. The cumulative release of Gentamicin at every time point was measured by normalizing the data based on the standard curve, using Excel.

F. Antibacterial assay

For both stem and cone, each experimental group (n=3) was coated with the optimised EPD setup and parameters. *S. Aureus* stain (49230, ATCC, US) was used to determine the antibacterial activity of the biomaterials. The specimens were brought in contact with tryptic soy broth (TSB) medium with 1% bacterial glucose suspension in the mid-log growth phase (OD600 = 0,01 107 bacteria /mL). The implants were incubated at 37 °C for 24h and continuously stirred using a rotation platform. The colony forming units (CFUs) were counted (plate counting) in duplo to quantify both adherent and planktonic bacteria at day 1 and day 7. For adherent bacteria, the specimens were rinsed three times using 2ml PBS, transferred to fresh PBS and sonicated for 1 min, to determine the CFU

count afterwards. For planktonic bacteria, 20 μL samples were taken from the incubation medium and used for CFU determination. The data were evaluated using Prism 8.2 and SPSS. To evaluate the inhibition zone, an *S. Aureus* strain (ATCC 49230) was grown on a blood agar plate (TSA) at 37 °C overnight. The culture was grown to log phase in fresh TSB. The bacterial suspension was diluted to 0,5 McFarland and evenly distributed over a TSA plate. The samples were placed on the plate and incubated at 37 °C overnight.

G. Cell viability assay

To measure the cell viability over a period of time, alamarBlue Cell Viability Reagent (Thermo Scientific MA, USA) was used. For every sample (n=3), 1 million MC3T3 osteoblast precursor cells were seeded on the implant specimen and incubated for 1 day in the alamarBlue reagent. After 1 day, the medium was changed and measured with a Fluoroskan Ascent FL multiplate reader (Thermo Labsystems, Helsinki) at an absorbance of 570 nm. This procedure was repeated every day over a period of 3 days to quantify the metabolic activity. Live/dead viability assay was performed for every AM experimental group (n=1) after 3 days of incubation at 37 °C to determine the cell adhesion and survival on the implant surface. Live cells were visualised with FITC (green) and dead cells using New Coccine (red), using a confocal microscope (LEICA TCS SP8-X, Ernst-Leitz-Str, Germany).

H. Statistical analyses

All data was analysed using SPSS and were presented by their mean ± standard deviation. One-way ANOVA with Tukey post-hoc correction was performed to compare the means between the different experimental groups in SPSS. The CFU data were first log-transformed and then a statistical analysis was performed to determine the antibacterial efficiency of the different experimental groups.

III. Results

A. Morphology of the AM and SB titanium surfaces

The SEM images (Fig. 2b.) show the structure and morphology of the AM and SB titanium surfaces. The AM and SB surfaces differ, as the partially melted titanium particles are removed after SB. The SEM images clearly show a change in surface roughness and morphology for SB compared to AM, since the surface between the partially melted titanium particles for the AM samples is very smooth without any scratches, whereas for the SB samples many small scratches can be seen. The thickness of the implant slightly decreases after shot blasting, due to the removal of the upper titanium layer from the sample.

B. Parameter optimization

After deposition of the coating on the AM samples using FITC with different voltage (V) and deposition time (t) parameters (fig. S3a+c.), the most homogeneous deposition was found using 10 V and 10 min. After addition of H_2O_2 in the colloid solution, a more homogeneous coating could be deposited for stem samples, since less uncoated

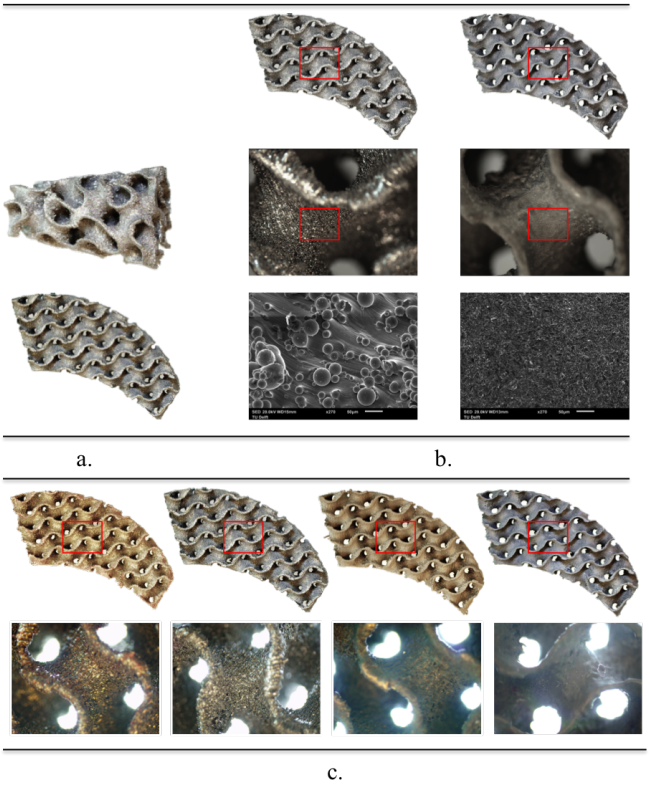

Fig. 2: (a) Macrograph of additively manufactured porous titanium specimens: Stem and cone shaped. (b) Macrograph and SEM pictures of the AM (Left) and SB (Right) stem specimens, top to bottom: 1X, 3X and 270X. (For cone: fig. S2) (c) Images of the optimised homogeneous coating on AM (left) and SB (right) stem specimens.

spots are visible on the implant surface (fig. S3b.). The cone sample shows no difference after addition of H_2O_2. After incorporation of the antibiotics, the gentamicin samples showed less uniformity compared to [Chi/Gel] and [Chi/Gel/Van], so parameters needed to be optimised for the gentamicin samples. Good results could be obtained for a voltage of 15 V and a deposition time of 15 min. Despite the use of H_2O_2, bubbles at the cathodic side of the [Chi/Gel/Gen] samples were observed during the EPD process. Table II. shows the optimised coating parameters that are used in this research to investigate biological response of the coating.

EDS mapping showed a highly increased elemental composition of Carbon for all coated samples, compared to [ASM] (n=1) (Table III). No increase for Nitrogen and Oxygen could be measured for all coated samples compared to [ASM]. However, the coated samples showed a considerable decrease of the Titanium and Aluminium elements, that exist in the titanium samples (Ti-6Al-4V) compared to the [ASM] samples. For all samples, Vanadium was not detectable when using area or point EDS mapping. In contrast, the EDS maps (fig. S5) did show Vanadium elements in the area measured for the [ASM] samples. Additionally, despite the fact that vancomycin Hydrochloride contains Cl (Chloride) and gentamicin Sulfate contains S (Sulfur), negligible values for Cl or S were detected.

The coating weight before and after coating deposition

	Sample (Stem/cone)	Surface AM/SB	Coating H_2O_2	Parameters V	t
1	ASM	AM	Yes	-	-
2	Chi/Gel	AM	Yes	10	10
3	Chi/Gel/Van	AM	Yes	10	10
4	Chi/Gel/Gen	AM	Yes	15	15
5	ASM	SB	Yes	-	-
6	Chi/Gel	SB	Yes	10	10
7	Chi/Gel/Van	SB	Yes	10	10
8	Chi/Gel/Gen	SB	Yes	15	15

TABLE II: Optimized parameters for the eight experimental groups.

Experimental group	Atomic concentration (%)							
	O	**C**	**N**	**Ti**	**Al**	**V**	**Cl**	**S**
SB-ASM	36,63	17,78	7,52	26,59	10,64	0,07	-	-
SB-Chi/Gel	29,60	63,64	3,35	2,27	0,94	0,08	-	-
SB-Chi/Gel/Van	30,81	65,46	3,48	0,08	0,04	0,02	0,11	-
SB-Chi/Gel/Gen	30,14	66,05	3,28	0,05	0,04	0	-	0,03

TABLE III: Atomic concentration of the different experimental groups measured at one representative area at 2200X magnification.

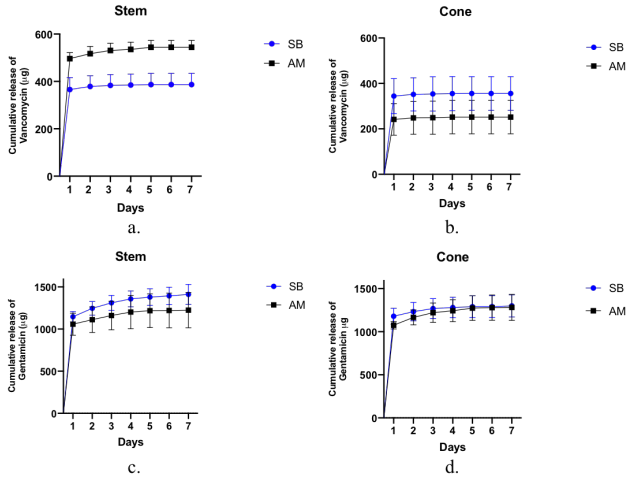

Fig. 3: Cumulative release profile measured over 7 days for vancomycin on stem (a) and cone (b) specimens, determined by UPLC and for gentamicin on stem (c) and cone (d) specimens, determined by UV-spectroscopy.

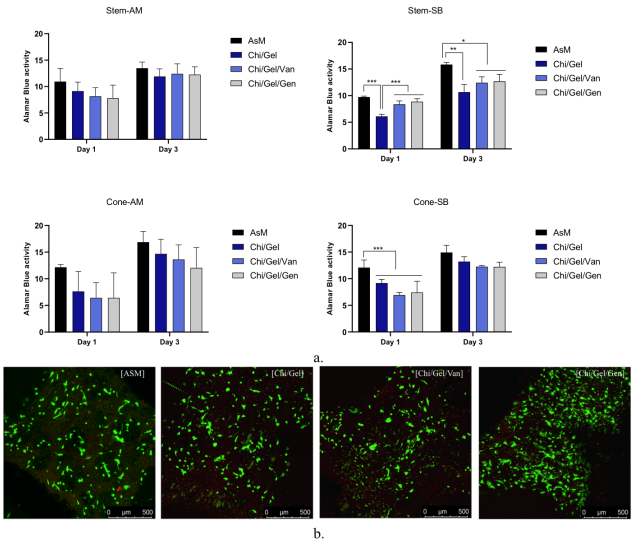

Fig. 4: a) MCT3T cell viability for the different experimental groups measured at day 1, and day 3 using AlamarBlue (n=3). b) Confocal Live/Dead fluorescence images of Stem-AM samples (10X) at day 3.

was determined, resulting in a coating weight with an average of 9 μg for both AM and SB stem samples and an average of 6 μg for both AM and SB cone samples (n=3).

C. Release profiles

The release profiles (Fig. 3a-d) clearly showed vancomycin and gentamicin release for both stem and cone. For all samples, in the first few hours to one day, a burst release is noticeable that is followed by a slowly sustained release over the next 7 days. For vancomycin release, the stem shows a higher release for the [AM-Chi/Gel/Van] samples compared to the [SB-Chi/Gel/Van], whether cone shows opposite results. The stem samples show a slightly higher release of vancomycin compared to the cone samples. For vancomycin release, a difference of around 100 μm could be detected between SB and AM samples. For both stem and cone coated with Gen, the difference in [AM-Chi/Gel/Gen] and [SB-Chi/Gel/Gen] groups were very small, with almost negligible increased values for SB samples. The amount of release for both stem and cone is comparable, but stem samples showed a slightly higher release for the SB samples.

D. Antibacterial effects

The antibacterial adherence for both vancomycin and gentamicin groups was significantly reduced compared to the [ASM] and [Chi/Gel] groups at day 1 for both cone and stem samples (Fig. 5a.). The adherent bacteria showed a significant decrease of Log 2 and the non-adherent bacteria (= planktonic bacteria) showed total eradication of *S. Aureus* after addition of vancomycin and gentamicin. The inhibition zone tests (Fig. 5b.) showed similar results. However, [Chi/Gel] and [ASM] were not able to kill bacteria upon contact, confirmed after both CFU and inhibition zone assays. The CFU results at day 7 show no significant difference between all experimental groups for both adherent as planktonic bacteria. This means that according to this data, the coated implants do not show increased antibacterial effect when samples are incubated in PBS for 7 days. However, the inhibition zone tests at

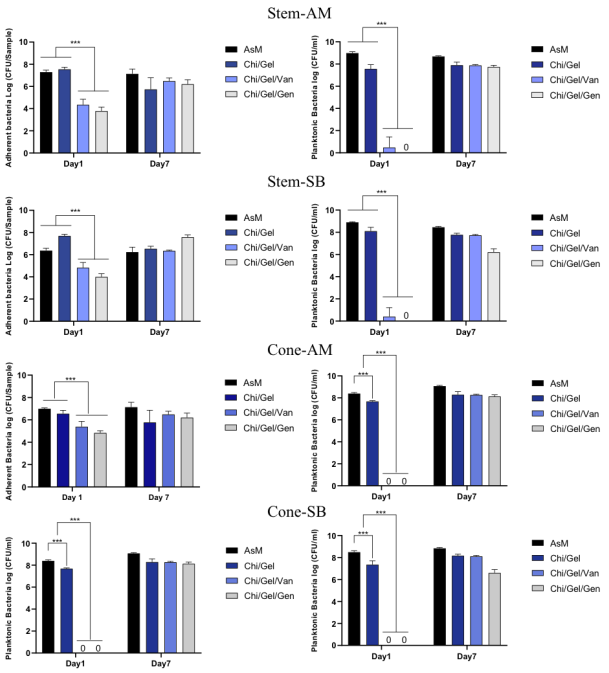

(a)

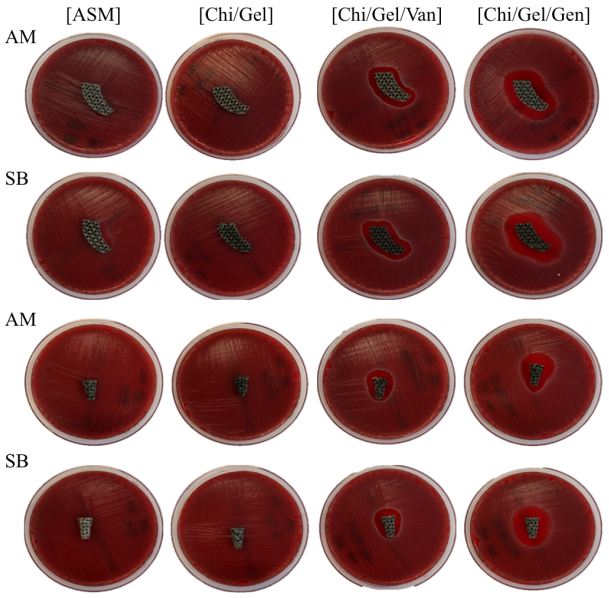

(b)

Fig. 5: (a) CFU's of the antibacterial killing effect at 1 day and day 7 for AM and SB specimens for both adherent and planktonic bacteria, measured for the different experimental groups (n=3). Representative images of the *S. Aureus* inhibition zones at day 1, for all experimental groups (b) (n=1) (Day 7:fig. S4

day 7 showed contradicting results. Eradication of bacteria was visible at day 7 for the Van and Gen groups compared to [ASM] and [Chi/Gel].

E. Cell viability

in vitro cell viability assay shows cell proliferation for every experimental group. A lower level of cytotoxicity for the [Chi/Gel] samples as well as [Chi/Gel/Van] was detected at day 1, only for the stem-SB samples. However, at day 3 cell proliferation could be noticed compared to day 1. The samples without coating showed no cytotoxicity and higher cell proliferation according to the alamarBlue assays (fig. 5a.). Live/dead assay at day 3 showed viable cells for all AM experimental groups, which is comparable to the alamarBlue data. No dead cells could be detected using this method. [Chi/Gel/Gen] demonstrates higher cell viability compared to the other groups, with almost fairly equally distributed cells. The [ASM], [Chi/Gel] and [Chi/Gel/Van] groups show less cells at day 3, however cells were present and equally distributed.

IV. Discussion

A. Problem statement and results

In this study, an attempt was made to solve the problem regarding IAI prevalence for complex orthopedic implants causing implant failure, by developing a method to deposit an antibacterial coating on titanium (Ti-6Al-4V) implants [2–4]. Prevention of biofilm formation, a problem that originates from surgery contamination during the first six hours after implantation, was the major focus of this research [1]. Nowadays, additively manufactured complex orthopedic implants are exclusively produced for the most critical situations, when no conventional approaches are applicable [14]. These additively manufactured metal implants are ideal, because of their specific bone mimicking mechanical properties, creating desirable host response and tissue regeneration to minimize bone resorption [13]. However, the procedures for implantation of these specific implants often require longer and more difficult surgical interventions, which is why patients are more susceptible for implant infection [3, 16]. It is therefore of great importance that an antibacterial coating is developed for complex implants. This may reduce the chance of revision on additively manufactured implants caused by IAIs. To co-deposit polymeric particles consisting of chitosan and gelatin, the technique of electrophoretic deposition (EPD) is used. EPD is known to be simple and fast, and therefore cost-effective, enabling the formation of a coating with adjustable thickness [30]. Antibiotics can be loaded in the polymeric particles formed in the colloid solution, creating an antibacterial efficient coating [24]. Release profiles for both vancomycin and gentamicin showed a burst release at day one which was followed by a sustained release until day seven. *In vitro* antibacterial assay resulted in a significant decrease in bacterial attachment for the vancomycin and gentamicin groups after day one. *In vitro* cell viability assay demonstrated no cytotoxicity. However, day three showed significantly higher pre-osteoblastic proliferation for the [ASM] group compared to the other experimental groups for the stem-SB samples. All other samples show no significant difference between the experimental groups. Live/dead assay on the other hand showed higher cell viability at day 3 for the [Chi/Gel/Gen] groups, nonetheless it confirmed that cell proliferation was present for all groups.

B. Electrophoretic deposition

In this research, EPD was applied in order to create a homogeneous antibacterial releasing coating on the complex implant specimen. Creating a coating on additively manufactured structures can be challenging, due to its

complexity and printing parameters. As explained before, the structure complexity can affect the surface roughness and morphology and additionally coating thickness and cell/bacterial adherence because of the underlying complex structures [18]. Decreased uniformity of a coating can negatively affect osseointegration and can increase bacterial infection susceptibility [19]. Spriano et al. (2018) showed that coating deposition on porous titanium involving heat decreased the uniformity of the coating, due to induced stress and delamination [31]. Next to that, since most antibiotics are not thermostable, deposition processes at room temperature are compulsory to enable the incorporation of a drug to create the bactericidal property [32, 33]. Hence, the application of a coating method that can be used at ambient temperatures was preferred over coating techniques that required elevated temperatures, such as chemical vapour deposition [18]. Furthermore, stability during electrochemical deposition methods is extremely important to create a coating with a desired thickness, uniformity and controlled release characteristics. Several techniques have gained increasing attention because of their promising and innovative nature including self-assembled monolayers, layer-by-layer assemblies or atomic transfer radical polymerization. However, the last two applications showed poor stability in ambient and physiological environments, making them unsuitable for this specific study [7]. The self-assembled monolayer method could be excluded for deposition of antibiotic incorporation, since big molecule incorporation is impossible for monolayer films [34]. Moreover, the use of this procedure for multilayer application is very time and material consuming [34]. More compatible and state-of-the-art methods for antibiotic loading are EPD, electrospraying and dip coating [16]. As explained before, EPD is known to be simple and fast, and thereby cost-effective, so therefore this effective method was chosen in this study to deposit the antibiotic loaded particles of chitosan and gelatin [7]. Earlier research showed that with optimised parameters, a uniform coating could be deposited on additively manufactured implants when using EPD [35]. Charged particles being well controlled and dispersed are key issues for a stable colloid suspension [19]. Optimisation of the parameters in this research (fig. S3a.) showed less homogeneity when voltages higher than 10V were applied. This could be explained by the fact that there is a threshold for the stability of a colloidal suspension, preventing deposition when the applied electric field surpasses excessive repulsion forces between particles [19]. Next to that, slower kinetics of particle migration will take place with lower voltages applied. Therefore, particles have more time to locate at a suitable position, creating higher uniformity [35]. Nonetheless, voltages lower than 10 V appeared to have a less uniform deposition of the [Chi/Gel] particles. So it seemed that the suspension was most stable at 10 V over a deposition period of 10 minutes. For gentamicin, a voltage of 15 V and a deposition time of 15 min were applied to create a stable deposition. A concentration of 1,0 mg/ml was used during our experiments for Gen, which is double the amount of Van (0,5 mg/ml). Therefore, higher EPD parameter values were needed to create stability during the EPD process [36]. These results indicate that when higher amounts of drugs are loaded into the Chi/Gel complexes, higher EPD parameters are needed to create the same deposition yield. Next to that, higher zeta potential is favourable for a colloid solution and a pH value between 3pH and 5,6pH seems ideal to create the polymeric complexes of chitosan and gelatin in MilliQ. Therefore, Acidic acid was added to the solution to create ideal suspension stability [19, 36].

C. Mechanical properties

To create ideal mechanical properties for the additively manufactured complex implants, shot blasting was applied on the stem and cone specimen. The SEM images of the Alumina shot blasted samples (Fig. 2b.) showed that the partially melted titanium particles were removed. An earlier study showed that shot blasted titanium surfaces decreased bacterial adhesion, preventing biofilm formation, compared to smooth surfaces or surfaces that are shot blasted with different powder particles [37, 38]. *S. Aureus* and *S. Epidermidis* attachment decreased with an increased surface roughness at nanoscale, while human osteoblast adhesion and proliferation was increased after surface treatment using shot blasting [38]. It appeared that surface roughness is inversely related to bacterial attraction [37, 38]. Additionally, the cellular surface of *S. Aureus* and *S. Epidermidis* is hydrophobic. Therefore, it was expected that the highest adhesion value would be obtained with smooth surfaces like the AM samples, since a lower hydrophilicity is visible for smooth surfaces compared to the Alumina shot blasted surfaces [37, 38]. This was confirmed by an earlier study, which showed higher bacterial attachment rates for smooth surfaces compared to shot blasting surfaces [37]. Benedetti et al. (2017) showed no relation between hydrophilicity and bacterial attachment, however suggested osteoblast adhesion corresponds to wettability and consequently to grain size, as grain size refinement was shown to increase hydrophilicity and thereby promoted osteoblast attachment and growth [39]. Not only biological parameters but also fatigue behaviour is shown to improve after shot blasting treatment. The reduction of partially melted titanium particles at the surface after shot blasting increased the fatigue resistance and crack formation at high cycle fatigue test by Benedetti et al. (2017) [39]. Hence, the low cost and fast post-processing shot blasting technique was preferred over other treatments like hot isostatic pressing and electropolishing [39]. It was decided to shot blast our samples with Alumina powder particles, since it showed preferable results over other powder particles used in other SB studies [37]. To detect the difference between AM and SB samples, both samples were used for *in vitro* assays. The SEM image of the AM sample 700X (fig. S2) shows a smooth surface in between the partially melted titanium particles. This could increase the bacterial attachment and decrease osteoblast adhesion and growth. The SB samples show roughness at nanoscale, where all partially melted titanium powder particles are removed. This should decrease bacterial attachment and reversely increase osteoblast adhesion and growth. After surface modification, solution and EPD parameter optimization was performed. Ideal EPD parameters were

found for the different experimental groups as shown in table II. Next to that, hydrogen peroxide (H_2O_2) addition to the colloidal solution showed increasing coating homogeneity (fig. S3b.). Because of electrolysis during the EPD process, H_2 bubbles were formed at the cathodic side, creating a local increase of pH ($2H_2O > 2H_2 + O_2$) [24]. Addition of H_2O_2 could decrease this bubble formation, thereby enabling the increase in homogeneity ($H_2O_2 + 2H^+ + 2^{e-} > 2H_2O$). This was observed during the EPD procedure for all samples, except for samples including gentamicin. Excessive bubble formation at the cathodic side could be observed, which could lead to porosity in the coating structure. A different coating structure was visible for the [SB-Chi/Gel/Gen] samples compared to the other shot blasted samples (fig. S3c.). Yet, no porosity could be detected, which is why it seems that the bubbles formed at the implant surface did not have significant effect on the coating homogeneity. gentamicin is shown to enhance the creation of hydrogen peroxide, so the addition of gentamicin in the colloid solution could probably block H_2O formation. This could explain the formation of bubbles at the cathodic side [40].

Chemical composition identification was assessed using EDS analysis for all experimental groups. Surface identification is important, since this upper layer interacts with the biological environment surrounding the implant, which can affect the biocompatibility and antibacterial effect [41]. Ti-6Al-4V is known as a biocompatible alloy, however the surface chemistry of additively manufactured titanium can differ from controversial surfaces and additionally coating composition has to be evaluated to ensure coating deposition on the implant sample [41]. The high presence of Carbon for all coated samples suggested that coating was deposited on the titanium surface (Table III), considering the high number of Carbon (C) ions in chitosan and gelatin. This is confirmed by the atomic decrease of Titanium (Ti) and Aluminium (Al), since coating deposition creates molecule layers making the Titanium surface less detectable. SEM operates with a layer around 1 μm or less, so the uppermost atomic layers will be analysed. However, Oxygen (O) and Nitrogen (N) did not show any increase in atomic concentration, despite the existence of these elements in not only the chitosan and gelatin molecules but also vancomycin and gentamicin (fig. S6). Light elements such as O and N are difficult to quantify using EDS due to limited sensitivity. Additionally, contamination can cause invalid values for the ubiquitous Oxygen, creating an error in this quantitative evaluation. Despite the inert atmosphere (with an Oxygen concentration below 50 ppm at which SLM operated), O could have been available during the printing process and could have reacted with Al and Ti, because of the high affinity to those elements. Higher chemical composition of TiO_2 was expected on the titanium surface, since Ti is more pronounced compared to Al. Hydrogen (H) could not be identified, because EDS mapping is related to identification of the K-shells. H only consists of one valence shell (one valence electron, that overlaps with signals from other atoms in EDS), so no K-shells could be measured [42]. Despite the fact that $\sim$4% Vanadium was expected for the [ASM] samples, this element was not detectable during EDS area evaluation [43]. Conversely, the EDS mapping (fig. S6) showed increased Vanadium concentration, suggesting the presence of Vanadium on the implant surface. Also C was detected at the surface of the [ASM] samples, which was probably caused by atmospheric contamination [41]. The samples coated with antibiotics could have shown small amounts of Sulfate (S) and Chloride (Cl), since vancomycin hydrochloride and gentamicin sulfate were used in this work. However, no S and Cl was detected. This could be caused by the lower presence of these ions (fig. S6), adding that spectrum noise cannot be neglected. Therefore, it could be possible that those elements are missed during this analysis. However, the EDS mapping (fig. S5) showed reasonable uniformity of the deposited coating in terms of chemical composite distribution, hence it could be suggested that coating was deposited on the implant surface, probably with a homogeneous distribution of molecule complexes.

D. Antibiotic loading

In this study, the two different drugs including vancomycin and gentamicin were loaded separately into the chitosan/gelatin complex to improve antibacterial activity. These water-soluble antibiotics are commonly used in clinic and have shown to decrease *S. Aureus* and *S. Epidermidis* colonization in earlier antibacterial coating studies [32]. Due to the polycation formation of the amino groups of chitosan and the Glycine amino acid in gelatin, which contains $-COO^-$ groups in acidic environments, polyelectrolyte complexes of chitosan and gelatin could be formed by means of electrostatic interaction, forming insoluble molecules [19].

Gentamicin and vancomycin are glycopeptide antibiotics and appear to have hydrophilic properties. The positively charged vancomycin and highly positively charged gentamicin form hydrogen and electrostatic bonds with the negatively charged gelatin, which is why particles of Chi/Gel loaded with antibiotics were formed in the colloid solution [44, 45]. To tune the amount of drug, either the drug to polymer ratio or the concentration of drug in the solution could be changed [7]. In this work, optimised amounts of drugs were used, that were derived from an earlier coating study [17]. To investigate the amount of drug released at specific time points, *in vitro* release tests were performed for both vancomycin and gentamicin. The *in vitro* release of vancomycin showed an initial burst release at day 1, followed by sustained release until day 7. Gelatin is a highly biodegradable protein that formed a complex with the less degradable chitosan to improve mechanical and biomedical properties including cell adhesion, shear bond strength and drug release [19]. Gelatin addition to the chitosan coating therefore enabled this burst release at day 1. Release behaviour of both AM and SB showed higher release for stem compared to cone specimen. After weighing the samples, more coating deposition yield was measured for the stem (9 mg) compared to cone (6 mg) samples. Stem specimen have a larger volume structure and thereby an increased surface area, so more coating deposition was possible. This could indicate the higher

vancomycin release for stem. Besides, a significant higher release of vancomycin from the SB samples for cone specimen could be noted, whereas stem samples showed opposite results. The effect of surface treatment on the release behaviour could be explained by the fact that SB surfaces are more hydrophilic compared to AM samples, creating more Van der Waals interactions with the composite coating. However, cone samples showed conflicting results, as well as both cone and stem specimen that were coated with [Chi/Gel/Gen]. More research should be assessed to make a clear statement about the effect of surface treatment on the release behaviour of antibiotic coatings. *In vitro* gentamicin release behaviour was comparable for stem and cone. Both profiles showed a burst release at day 1, followed by sustained release until day 7, similar to the release profiles of vancomycin. Given that 9 mg of coating is deposited including approximately 30% of gentamicin, one third of all gentamicin was released after one day. This is favourable in case of fighting peri implant site infections, since bacteria need to be killed immediately upon contact after implantation. However, bacteria entering the body in a later stadium will have a smaller chance of being killed by gentamicin in the implant environment due to antibiotic release, since there is a slow release of antibiotics over the next 7 days.

The *in vitro* cell viability assays shows favourable adhesion and growth of the pre-osteoblastic cells over the 3 days measured. Spreading of cells over the implant surface is detected with live/dead assay, leading to the conclusion that all experimental groups show no toxicity and enhanced osteogenic differentiation. The composite coating loaded with gentamicin showed a higher number of cells compared to the other experimental groups, suggesting that the [Chi/Gel/Gen] coating promotes cell proliferation. The reason for this might be the increase of hydrophilicity when using gentamicin (because of its amino side chains), since osteoblastic differentiation is enhances by hydrophilicity and surface roughness [46]. *In vitro* alamarBlue assay shows that for the stem-SB samples, higher values could be measured for the [ASM] group. This suggested that cells prefer the SB surface over a coated surface. Nano-roughness is favourable for osteoblastic differentiation, so it could be said that cell proliferation was enhanced by the SB surface [38].

At last, *in vitro* antibacterial efficiency showed significant decrease of the colony-forming unit of adherent bacteria and planktonic bacteria for the experimental groups containing antibiotics. This confirmed the bactericidal effect of a vancomycin and gentamicin release coating. Despite the antibacterial properties of chitosan, no significant difference could be detected between the [ASM] and [Chi/Gel] groups, indicating that the [Chi/Gel] coating did not create any antibacterial effect [21]. Earlier research confirmed this result, showing that a [Chi/Gel] coating did not kill *S. Aureus* without antibiotic loading [24]. Next to that, the surface roughness should decrease the attachment of bacteria according to literature. However, no significant antibacterial effect was found between the AM and SB groups. Since SB enhances the mechanical properties of the implants, it is preferable to shot blast the titanium implants, since it does not decrease antibacterial efficiency. Hence, it is thought that antibiotic loading could be the only effective possibility to increase the antibacterial effect of the titanium samples in this setup. Furthermore, significantly more planktonic bacteria were eradicated compared to adherent bacteria. Nearly all planktonic bacteria were gone after one day, whereas the biofilm forming bacteria could still be detected in all experimental groups, confirming that total eradication was not possible. Possibly, bacteria could colonise at non-coated areas on the implant surface or areas that contained less antibiotics. More uniformity quantification could be performed such as cross-section measurements, to determine the exact coating thickness and uniformity of the coating at different locations [17]. However, inhibition zone results did show total bacteria eradication for the vancomycin and gentamicin groups, not only at day 1 but also at day 7. Yet, according to the CFU results, the samples were not able to kill bacteria upon contact after 7 days. The release profile shows that after 7 days only slow sustained release of vancomycin or gentamicin is visible, so the antibacterial effect of the antibiotic release coatings will be significantly lower after 7 days. Earlier research showed that a [Chi/Gel] coating including vancomycin was able to eradicate all adherent bacteria at day 1 [17]. The difference in this research compared to our work exists in the use of implant specimen, because despite the fact that additively manufactured porous samples were used, no complex shapes were included in their work. The complex shapes of patient specific implants, comparable to the implant specimen used in our study, will remain the biggest challenges to overcome the problem regarding bacterial colonization. It is clear that a perfectly uniform antibacterial coating is not yet achieved for these specific shapes. Hence, more research is needed to fully accomplish eradication of adherent bacteria *in vitro*. Difference in antibiotic use was detected, since gentamicin showed a bigger inhibition zone against *S. Aureus* compared to vancomycin at both day 1 and day 7 for stem and cone. However, double the amount of gentamicin was used in this study, which makes comparison between these antibiotics difficult.

Because of the new technologies and techniques for which no strict guidelines or protocols exist, the risk of missteps cannot be neglected. Nevertheless, significant decrease could be detected for the antibiotic loaded coatings. Therefore, electrophoretic deposition of a chitosan/gelatin based coating loaded with antibiotics to create a burst release which can fight peri implant infection seems a promising solution for patient specific orthopedic implants.

E. Clinical perspective

Electrophoretic deposition as a method to deposit an antibiotic loaded coating seems a promising, simple and cost-effective way to eradicate bacterial infections. However, *in vivo* large animal model study is suggested to examine the working mechanism of this coating for complex titanium implants in clinic. Regulations and guidelines should be explored and set for this method, to optimise the working mechanism, effectiveness and additionally

to create a simple in clinic scenario that is convenient for surgeons, since their preference for conventional (less effective) approaches will otherwise remain. In clinic, less porous shapes will be used as complex implants, because implant revision will be impossible when full osseointegration occurs. However, to investigate deposition of the antibacterial coating on such structures, methods including most complex implant shapes must be employed *in vitro* as well as *in vivo* in next studies.

Nowadays, *S. Aureus* and *S. Epidermidis* are the cause of increasing rates regarding antibiotic resistance. *Methicillin-resistant S. Aureus (MRSA)*, causing early infection and *Methicillin-sensitive S. Aureus (MSSA)*, causing late infection, are the two main examples of these antibiotic resistant bacteria. Despite the facts that antibiotics based on glycopeptides can eradicate Methicillin resistant bacteria, the aforementioned bacteria and also *S. Epidermidis* were reported to be developing resistance towards gentamicin [1]. As a result of natural selection, antibiotics remove drug-sensitive competitors, leaving resistant bacteria behind for reproduction [47]. At the moment, the prevalence of MRSA in Europe is very low. Especially in the Netherlands, less than 1% of *S. Aureus* infections is caused by *MRSA* [48]. However, in future, antibacterial resistance should be taken into account when developing coatings including gentamicin or other antibiotics having risk of antibacterial resistance, since resistance can increase over time.

V. Conclusion

A chitosan/gelatin composite coating loaded with antibiotics has been successfully deposited on the complex implants by means of EPD. All experimental groups showed a stable and uniform coating on the additively manufactured complex titanium implants. A burst release of antibiotics resulted in high biodegradability of the coating, due to the gelatin incorporation in the particle complexes, being favourable for peri implant infection eradication. Difference in surface roughness did not show significant effect on coating deposition, release behaviour, cell proliferation or antibacterial activity. This is why shot blasting is suggested in future studies, since it has been shown to increase the mechanical behaviour of the implant surface. Gentamicin coating showed higher pre-osteoblastic proliferation compared to the other experimental groups, possibly due to its high hydrophilicity. This could suggest that a gentamicin loaded coating could enhance the cell viability. Addition of antibiotics in the coating greatly influenced the antibacterial behaviour, decreasing biofilm formation and eliminating planktonic bacteria. Hereby, first steps were made towards an antibacterial coating method developed for patient specific additively manufactured complex metal implants, to avoid implant revision.

VI. Acknowledgement

The collaboration project is co-funded by the PPP. Allowance made available by Health∼Holland, Top Sector Life Sciences Health, to LSHM18026 to stimulate public-private partnerships. I would gratefully acknowledge F. Jahanmard for her assistance in the lab and A. Majed for his technical assistance. Furthermore, I wish to thanks S.M. Ahmadi from Amber Implants (Delft) for providing us with the additively manufactured implant samples and assisting me on a technical level.

References

[1] Carla Renata Arciola, Davide Campoccia, and Lucio Montanaro. Implant infections: adhesion, biofilm formation and immune evasion. *Nature Reviews Microbiology*, 16(7):397, 2018.

[2] Dutch Arthroplasty Register. Online lroi annual report 2018, 2018.

[3] Ma Geetha, Ashok K Singh, Rajamanickam Asokamani, and Ashok K Gogia. Ti based biomaterials, the ultimate choice for orthopaedic implants–a review. *Progress in materials science*, 54(3):397–425, 2009.

[4] Steven Kurtz, Kevin Ong, Edmund Lau, Fionna Mowat, and Michael Halpern. Projections of primary and revision hip and knee arthroplasty in the united states from 2005 to 2030. *JBJS*, 89(4):780–785, 2007.

[5] Vinay K Aggarwal, Hooman Bakhshi, Niklas Unter Ecker, Javad Parvizi, Thorsten Gehrke, and Daniel Kendoff. Organism profile in periprosthetic joint infection: pathogens differ at two arthroplasty infection referral centers in europe and in the united states. *The journal of knee surgery*, 27(05):399–406, 2014.

[6] F Ordikhani, E Tamjid, and A Simchi. Characterization and antibacterial performance of electrodeposited chitosan–vancomycin composite coatings for prevention of implant-associated infections. *Materials Science and Engineering: C*, 41:240–248, 2014.

[7] Sadra Bakhshandeh and Saber Amin Yavari. Electrophoretic deposition: a versatile tool against biomaterial associated infections. *Journal of Materials Chemistry B*, 6(8):1128–1148, 2018.

[8] Amir A Zadpoor and Jos Malda. Additive manufacturing of biomaterials, tissues, and organs, 2017.

[9] S Amin Yavari, SM Ahmadi, J Van der Stok, Ruben Wauthlé, AC Riemslag, Michael Janssen, Jan Schrooten, H Weinans, and AA Zadpoor. Effects of bio-functionalizing surface treatments on the mechanical behavior of open porous titanium biomaterials. *Journal of the mechanical behavior of biomedical materials*, 36:109–119, 2014.

[10] Xiaojian Wang, Shanqing Xu, Shiwei Zhou, Wei Xu, Martin Leary, Peter Choong, M Qian, Milan Brandt, and Yi Min Xie. Topological design and additive manufacturing of porous metals for bone scaffolds and orthopaedic implants: A review. *Biomaterials*, 83:127–141, 2016.

[11] FSL Bobbert, K Lietaert, Ali Akbar Eftekhari, B Pouran, SM Ahmadi, H Weinans, and AA Zadpoor. Additively manufactured metallic porous biomaterials based on minimal surfaces: A unique combination of topological, mechanical, and mass transport properties. *Acta biomaterialia*, 53:572–584, 2017.

[12] Ingmar AJ van Hengel, Martijn Riool, Lidy E Fratila-Apachitei, Janneke Witte-Bouma, Eric Farrell, Amir A Zadpoor, Sebastian AJ Zaat, and Iulian Apachitei. Selective laser melting porous metallic implants with immobilized silver nanoparticles kill and prevent biofilm formation by methicillin-resistant staphylococcus aureus. *Biomaterials*, 140: 1–15, 2017.

[13] Amir A Zadpoor. Bone tissue regeneration: the role of scaffold geometry. *Biomaterials science*, 3(2): 231–245, 2015.

[14] Koen Willemsen, Razmara Nizak, Herke Jan Noordmans, René M Castelein, Harrie Weinans, and Moyo C Kruyt. Challenges in the design and regulatory approval of 3d-printed surgical implants: a two-case series. *The Lancet Digital Health*, 1(4): e163–e171, 2019.

[15] Leonardo Ciocca, Simona Mazzoni, Massimiliano Fantini, Franco Persiani, Claudio Marchetti, and Roberto Scotti. Cad/cam guided secondary mandibular reconstruction of a discontinuity defect after ablative cancer surgery. *Journal of Cranio-Maxillofacial Surgery*, 40(8):e511–e515, 2012.

[16] Ori Geuli, Noah Metoki, Tal Zada, Meital Reches, Noam Eliaz, and Daniel Mandler. Synthesis, coating, and drug-release of hydroxyapatite nanoparticles loaded with antibiotics. *Journal of Materials Chemistry B*, 5(38):7819–7830, 2017.

[17] S Bakhshandeh, Z Gorgin Karaji, K Lietaert, Ad C Fluit, CHE Boel, H Charles Vogely, T Vermonden, Wim E Hennink, H Weinans, Amir A Zadpoor, et al. Simultaneous delivery of multiple antibacterial agents from additively manufactured porous biomaterials to fully eradicate planktonic and adherent staphylococcus aureus. *ACS applied materials & interfaces*, 9(31):25691–25699, 2017.

[18] Aaqil Rifai, Nhiem Tran, Desmond W Lau, Aaron Elbourne, Hualin Zhan, Alastair D Stacey, Edwin LH Mayes, Avik Sarker, Elena P Ivanova, Russell J Crawford, et al. Polycrystalline diamond coating of additively manufactured titanium for biomedical applications. *ACS applied materials & interfaces*, 10 (10):8474–8484, 2018.

[19] Egemen Avcu, Fatih E Baştan, Hasan Z Abdullah, Muhammad A Ur Rehman, Yasemin Yıldıran Avcu, and Aldo R Boccaccini. Electrophoretic deposition of chitosan-based composite coatings for biomedical applications: A review. *Progress in Materials Science*, 2019.

[20] Saber Amin Yavari, Loek Loozen, Fernanda L Paganelli, Sadra Bakhshandeh, Karel Lietaert, Joris A Groot, Ad C Fluit, CHE Boel, Jacqueline Alblas, Henry C Vogely, et al. Antibacterial behavior of additively manufactured porous titanium with nanotubular surfaces releasing silver ions. *ACS applied materials & interfaces*, 8(27):17080–17089, 2016.

[21] Kapil D Patel, Rajendra K Singh, Eun-Jung Lee, Cheol-Min Han, Jong-Eun Won, Jonathan C Knowles, and Hae-Won Kim. Tailoring solubility and drug release from electrophoretic deposited chitosan–gelatin films on titanium. *Surface and coatings technology*, 242:232–236, 2014.

[22] Changjun Han, Yao Yao, Xian Cheng, Jiaxin Luo, Pu Luo, Qian Wang, Fang Yang, Qingsong Wei, and Zhen Zhang. Electrophoretic deposition of gentamicin-loaded silk fibroin coatings on 3d-printed porous cobalt–chromium–molybdenum bone substitutes to prevent orthopedic implant infections. *Biomacromolecules*, 18(11):3776–3787, 2017.

[23] Fatemehsadat Pishbin, Viviana Mourino, Sabrina Flor, Stefan Kreppel, Vehid Salih, Mary P Ryan, and Aldo R Boccaccini. Electrophoretic deposition of gentamicin-loaded bioactive glass/chitosan composite coatings for orthopaedic implants. *ACS applied materials & interfaces*, 6(11):8796–8806, 2014.

[24] Jiankang Song, Qiang Chen, Yang Zhang, Mani Diba, Eva Kolwijck, Jinlong Shao, John A Jansen, Fang Yang, Aldo R Boccaccini, and Sander CG Leeuwenburgh. Electrophoretic deposition of chitosan coatings modified with gelatin nanospheres to tune the release of antibiotics. *ACS applied materials & interfaces*, 8(22):13785–13792, 2016.

[25] Ziqiang Kong, Mengfei Yu, Kui Cheng, Wenjian Weng, Huiming Wang, Jun Lin, Piyi Du, and Gaorong Han. Incorporation of chitosan nanospheres into thin mineralized collagen coatings for improving the antibacterial effect. *Colloids and Surfaces B: Biointerfaces*, 111:536–541, 2013.

[26] SM Ahmadi, R Kumar, EV Borisov, R Petrov, S Leeflang, Y Li, N Tümer, R Huizenga, C Ayas, AA Zadpoor, et al. From microstructural design to surface engineering: A tailored approach for improving fatigue life of additively manufactured metabiomaterials. *Acta biomaterialia*, 83:153–166, 2019.

[27] Aldo R Boccaccini and Igor Zhitomirsky. Application of electrophoretic and electrolytic deposition techniques in ceramics processing. *Current Opinion in Solid State and Materials Science*, 6(3):251–260, 2002.

[28] Ilaria Corni, Mary P Ryan, and Aldo R Boccaccini. Electrophoretic deposition: From traditional ceramics to nanotechnology. *Journal of the European Ceramic Society*, 28(7):1353–1367, 2008.

[29] Yifeng Wang, Xuecheng Guo, Ruihao Pan, Di Han, Tao Chen, Zenghua Geng, Yanfei Xiong, and Yanjun Chen. Electrodeposition of chitosan/gelatin/nanosilver: a new method for constructing biopolymer/nanoparticle composite films with conductivity and antibacterial activity. *Materials Science and Engineering: C*, 53:222–228, 2015.

[30] Ashkan Bigham, Ahmad Saudi, Mohammad Rafienia, Shahram Rahmati, Hassan Bakhtiyari, Fatemeh Salahshouri, Mansoureh Sattary, and SA Hassanzadeh-Tabrizi. Electrophoretically deposited mesoporous magnesium silicate with ordered nanopores as an antibiotic-loaded coating on surface-modified titanium. *Materials Science and Engineering: C*, 96:765–775, 2019.

[31] Silvia Spriano, Seiji Yamaguchi, Francesco Baino,

and Sara Ferraris. A critical review of multifunctional titanium surfaces: New frontiers for improving osseointegration and host response, avoiding bacteria contamination. *Acta biomaterialia*, 79:1–22, 2018.

[32] H Chouirfa, H Bouloussa, V Migonney, and C Falentin-Daudré. Review of titanium surface modification techniques and coatings for antibacterial applications. *Acta biomaterialia*, 2018.

[33] B Tuleubaev, S Ahmetova, A Koshanova, A Rudenko, and E Tashmetov. Heat stability of the antimicrobial activity of antibiotics after high temperature exposure. In *Orthopaedic Proceedings*, volume 100, pages 34–34. The British Editorial Society of Bone & Joint Surgery, 2018.

[34] Joao Borges and Joao F Mano. Molecular interactions driving the layer-by-layer assembly of multilayers. *Chemical reviews*, 114(18):8883–8942, 2014.

[35] Ekaterina A Chudinova, Maria A Surmeneva, Alexander S Timin, Timofey E Karpov, Alexandra Wittmar, Mathias Ulbricht, Anna Ivanova, Kateryna Loza, Oleg Prymak, Andrey Koptyug, et al. Adhesion, proliferation, and osteogenic differentiation of human mesenchymal stem cells on additively manufactured ti6al4v alloy scaffolds modified with calcium phosphate nanoparticles. *Colloids and Surfaces B: Biointerfaces*, 176:130–139, 2019.

[36] YY Shi, M Li, Q Liu, ZJ Jia, XC Xu, Y Cheng, and YF Zheng. Electrophoretic deposition of graphene oxide reinforced chitosan–hydroxyapatite nanocomposite coatings on ti substrate. *Journal of Materials Science: Materials in Medicine*, 27(3):48, 2016.

[37] A Rodríguez-Hernández, E Espinar, JM Llamas, JM Barrera, and FJ Gil. Alumina shot-blasted particles on commercially pure titanium surfaces prevent bacterial attachment. *Materials Letters*, 92:42–44, 2013.

[38] Sara Bagherifard, Daniel J Hickey, Alba C de Luca, Vera N Malheiro, Athina E Markaki, Mario Guagliano, and Thomas J Webster. The influence of nanostructured features on bacterial adhesion and bone cell functions on severely shot peened 316l stainless steel. *Biomaterials*, 73:185–197, 2015.

[39] M Benedetti, E Torresani, M Leoni, V Fontanari, M Bandini, Cecilia Pederzolli, and Cristina Potrich. The effect of post-sintering treatments on the fatigue and biological behavior of ti-6al-4v eli parts made by selective laser melting. *Journal of the mechanical behavior of biomedical materials*, 71:295–306, 2017.

[40] Patrick D Walker, Yousri Barri, and Sudhir V Shah. Oxidant mechanisms in gentamicin nephrotoxicity. *Renal failure*, 21(3-4):433–442, 1999.

[41] Michaela Fousová, Dalibor Vojtěch, Jiří Kubásek, Eva Jablonská, and Jaroslav Fojt. Promising characteristics of gradient porosity ti-6al-4v alloy prepared by slm process. *Journal of the mechanical behavior of biomedical materials*, 69:368–376, 2017.

[42] Nenad Stojilovic. Why can't we see hydrogen in x-ray photoelectron spectroscopy? *Journal of Chemical Education*, 89(10):1331–1332, 2012.

[43] Marta Kiel, Janusz Szewczenko, Jan Marciniak, and Katarzyna Nowińska. Electrochemical properties of ti-6al-4v eli alloy after anodization. In *Information Technologies in Biomedicine*, pages 369–378. Springer, 2012.

[44] Jiankang Song, Jim CE Odekerken, Dennis WPM Löwik, Paula M López-Pérez, Tim JM Welting, Fang Yang, John A Jansen, and Sander CG Leeuwenburgh. Influence of the molecular weight and charge of antibiotics on their release kinetics from gelatin nanospheres. *Macromolecular bioscience*, 15(7): 901–911, 2015.

[45] Azam Ahangari, Mojtaba Salouti, Zahra Heidari, Ali Reza Kazemizadeh, and Ali Asghar Safari. Development of gentamicin-gold nanospheres for antimicrobial drug delivery to staphylococcal infected foci. *Drug delivery*, 20(1):34–39, 2013.

[46] Yu Zhang, Oleh Andrukhov, Simon Berner, Michael Matejka, Marco Wieland, Xiaohui Rausch-Fan, and Andreas Schedle. Osteogenic properties of hydrophilic and hydrophobic titanium surfaces evaluated with osteoblast-like cells (mg63) in coculture with human umbilical vein endothelial cells (huvec). *dental materials*, 26(11):1043–1051, 2010.

[47] C Lee Ventola. The antibiotic resistance crisis: part 1: causes and threats. *Pharmacy and therapeutics*, 40(4):277, 2015.

[48] Rijksinstituut voor volksgezondheid en milieu, infectieziekten bulletin. https://magazines.rivm.nl/2018/04/infectieziekten-bulletin-0, 2018, 29(10). Accessed: 06-05-2019.

[49] Merck, sigma-aldrich chitosan. https://www.sigmaaldrich.com/catalog/product/aldrich/448869?lang=en&region=NL, 2019. Accessed: 27-09-2019.

[50] Merck, sigma-aldrich gelatin methacryloyl. https://www.sigmaaldrich.com/catalog/product/aldrich/900496?lang=en&region=NL, 2019. Accessed: 27-09-2019.

[51] Biovision, vancomycin hydrochloride. https://www.biovision.com/vancomycin-hydrochloride.html, 2018. Accessed: 27-09-2019.

[52] Canvax, gentamicin sulfate. https://lifescience.canvaxbiotech.com/product/gentamicin-sulfate/, 2019. Accessed: 27-09-2019.

VII. SUPPLEMENTARY

a. b.

Fig. S1: a) 50 micron Alumina (Al_2O_3) abrasive used for shot blasting. b) Schematic shot blasting setup.

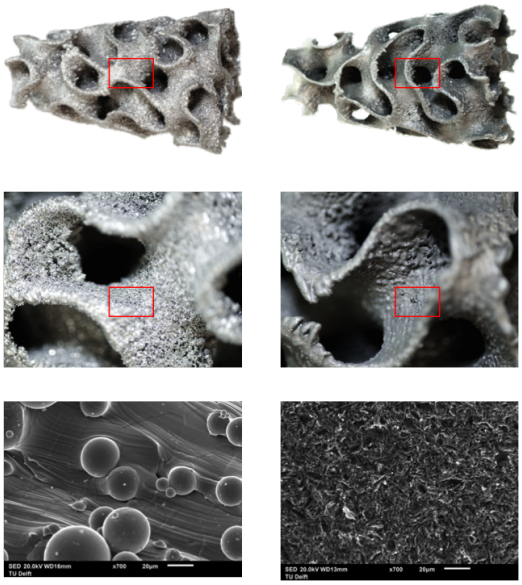

Fig. S2: Macrograph and SEM pictures of the as manufactured (Left) and shot blasted (Right) cone specimens, top to bottom: 1X, 3X and 700X

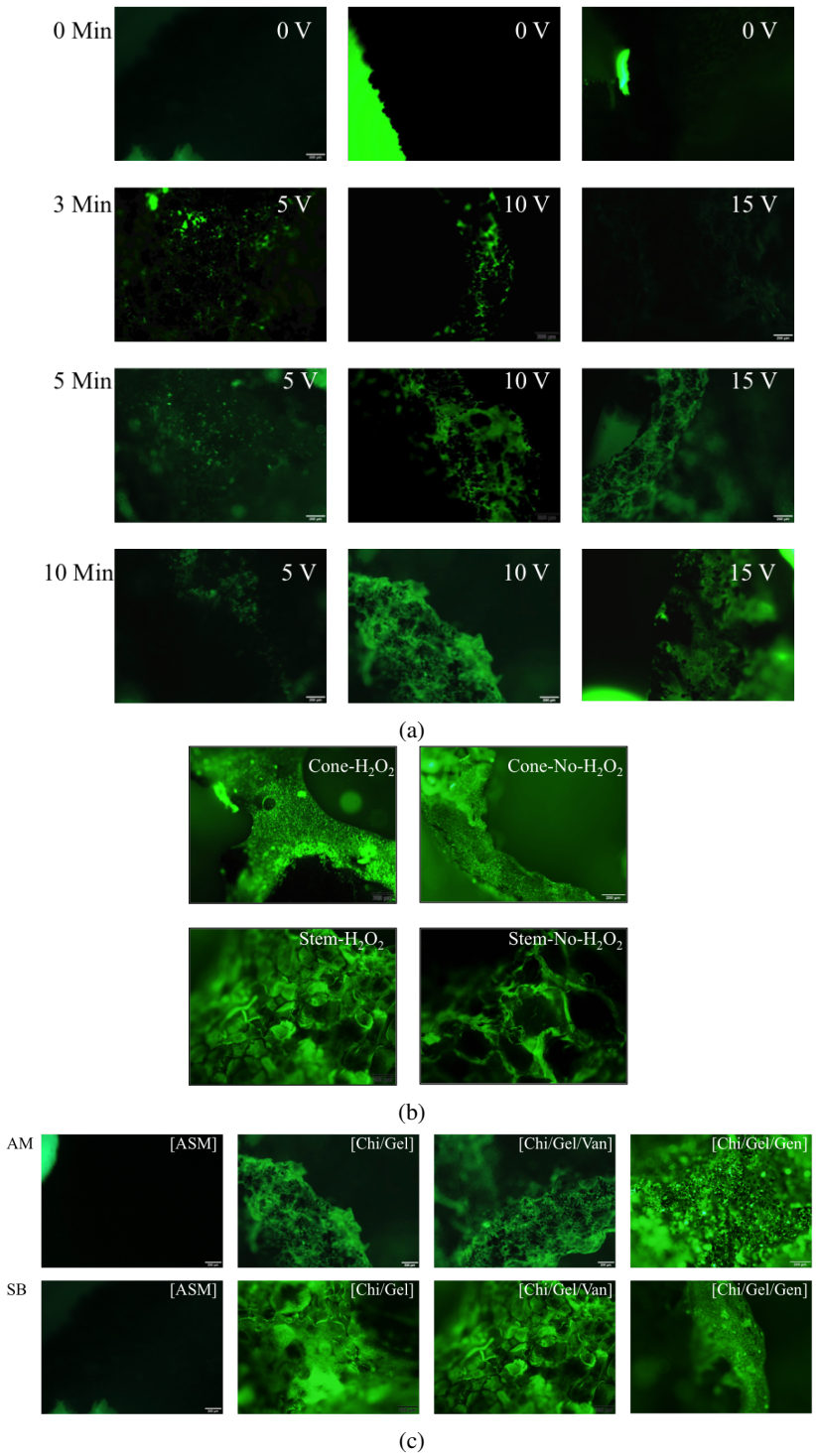

Fig. S3: a) Fluorescent images (FITC) of the optimization of coating parameters for AM cone and stem: deposition time and voltage. b) Fluorescent images (FITC) of the optimised coating with and without addition of H_2O_2 in the suspension on SB samples (Top: cone, Bottom: stem). c) Fluorescent images of the optimised coating for the different experimental groups (Top: AM, bottom: SB).

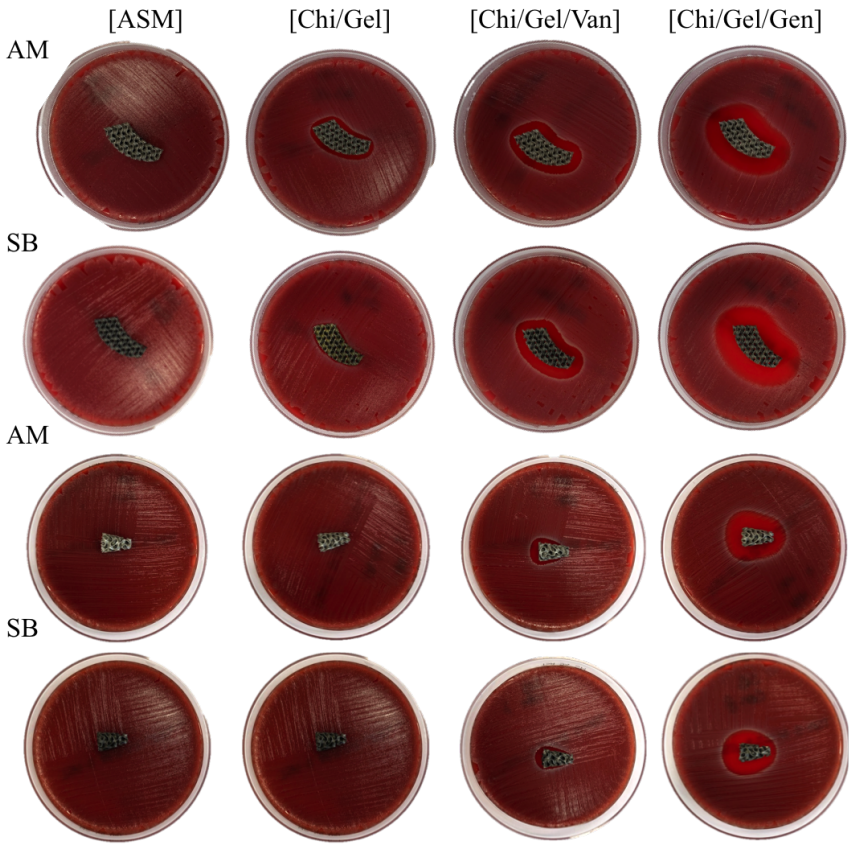

Fig. S4: a) CFU's of the antibacterial killing effect after 7 days for AM and SB stem specimens for adherent and planktonic bacteria measured for different coating composition groups (n=3). Representative images of the inhibition zones for the same groups (b) (n=1).

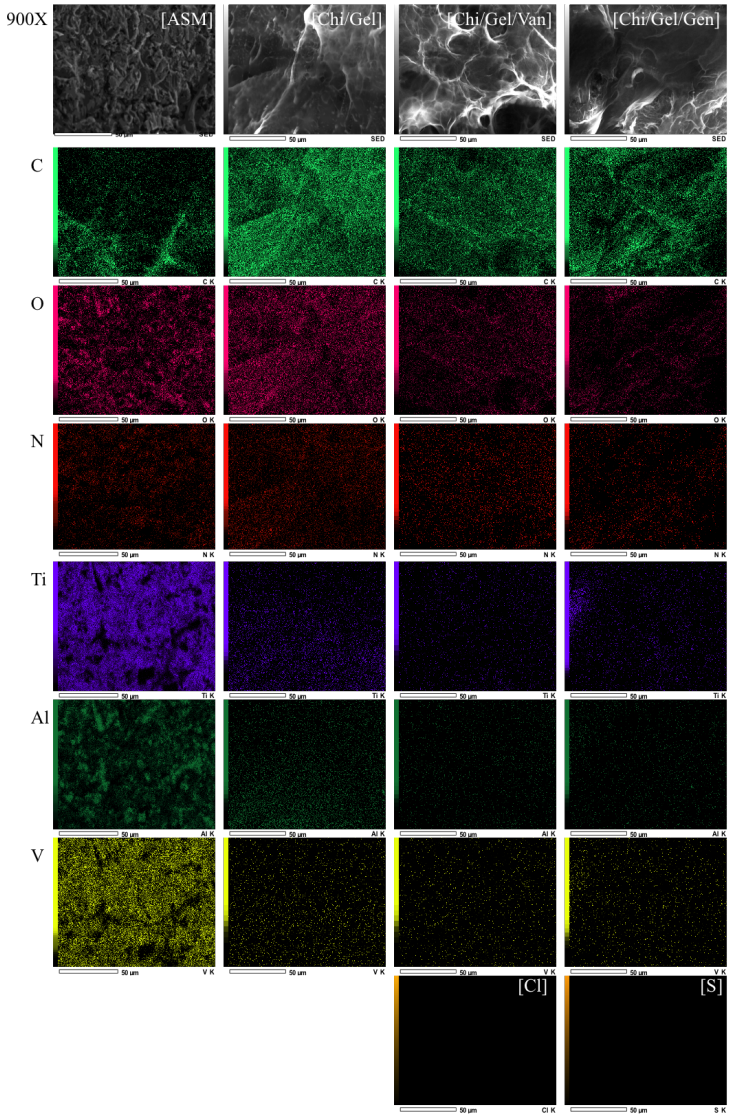

Fig. S5: EDS map [SB-ASM], [SB-Chi/Gel], [SB-Chi/Gel/Van], [SB-Chi/Gel/Gen] for atoms existing at the surface of the titanium implants (Ti-6Al-4V), the [Chi/Gel] complex coating (C, O, N) and the loaded antibiotics vancomycin hydrochloride (Cl) and gentamicin Sulphate (S)

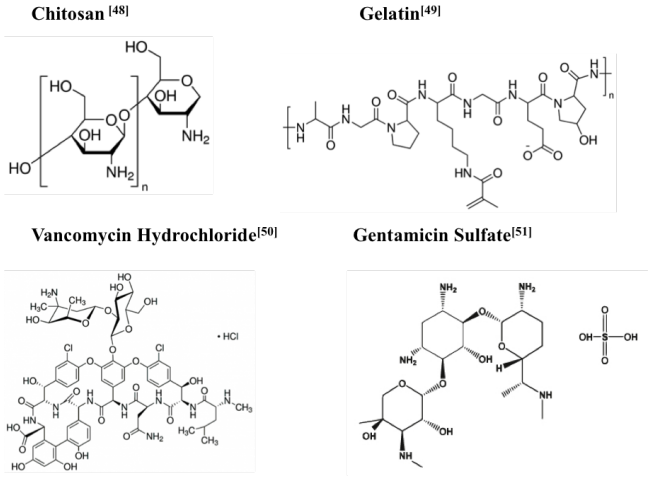

Fig. S6: EDS map [SB-ASM], [SB-Chi/Gel], [SB-Chi/Gel/Van], [SB-Chi/Gel/Gen] for atoms existing at the surface of the titanium implants (Ti-6Al-4V), the chitosan/gelatin complex coating (C, O, N) and the loaded antibiotics vancomycin hydrochloride (Cl) and gentamicin Sulphate (S) [49–52]